Wavelength-dependent nonsequential double ionization of magnesium by intense femtosecond laser pulses

HuiPeng Kang,[1,2,3,*] Shi Chen,[4,5] YanLan Wang,[3] Wei Chu,[6] JinPing Yao,[6] Jing Chen,[5,7] XiaoJun Liu,[3] Ya Cheng,[6,8] and ZhiZhan Xu[6]

[1]*Institute of Optics and Quantum Electronics, Friedrich Schiller University Jena, Max-Wien-Platz 1, 07743 Jena, Germany*

[2]*Helmholtz Institut Jena, Frötbelstieg 3, 07743 Jena, Germany*

[3]*State Key Laboratory of Magnetic Resonance and Atomic and Molecular Physics, Wuhan Institute of Physics and Mathematics, Chinese Academy of Sciences, Wuhan 430071, China*

[4]*School of Physics, Peking University, Beijing 100871, China*

[5]*HEDPS, Center for Applied Physics and Technology, Peking University, Beijing 100871, China*

[6]*State Key Laboratory of High Field Laser Physics, Shanghai Institute of Optics and Fine Mechanics, Chinese Academy of Sciences, Shanghai 201800, China*

[7]*Institute of Applied Physics and Computational Mathematics, P.O. Box 8009, Beijing 100088, China*

[8]*State Key Laboratory of Precision Spectroscopy, East China Normal University, Shanghai 200062, China*

(Received 28 May 2019; revised manuscript received 8 August 2019; published 5 September 2019)

We report on a systematic investigation of wavelength scaling strong-field double ionization of Mg in intense laser fields. A significant decrease of nonsequential double ionization (NSDI) yield with increasing wavelength from 800–2000 nm is observed. Our data is well reproduced by a three-dimensional Monte Carlo simulation considering recollision impact excitation cross section. We demonstrate that the NSDI of Mg mainly occurs via the first ionic excited state $Mg^{+*}(3p^2P_{3/2,1/2})$ pumped by returning electron impact process. The recollision impact direct ionization pathway plays a minor role here. The wavelength dependence of the NSDI ratio is due to the recollision energy-dependent excitation cross section as well as the electron wave packet diffusion effects, both sensitively depending on the wavelength. Our work represents a step towards strong-field double ionization experiments on Mg in the long wavelength limit and sheds light on the NSDI mechanism of alkaline-earth metal atoms.

DOI: 10.1103/PhysRevA.100.033403

I. INTRODUCTION

Regarded as one dramatic manifestation of dynamical electron-electron correlation in nature, strong laser field-induced nonsequential double ionization (NSDI) has continued to receive intense experimental and theoretical attention (for reviews, see Refs. [1,2]). This phenomenon was discovered to exhibit a strong enhancement in the double ion yield versus intensity curve, i.e., a characteristic "knee" structure, over predictions by the sequential tunneling theory [3]. This knee structure has been observed in all rare-gas atoms [4–6] and some molecules [7–10] over a range of intermediate laser intensities. A large number of kinematically complete experiments, which were performed mainly on rare-gas atoms [11–14], have offered convincing evidences that the underlying mechanism of NSDI is the quasiclassical recollision model [15]. In this model, after tunneling through the distorted Coulomb potential, the first electron may be accelerated and driven back to its parent ion by the oscillating laser field, where it can free a second electron by inelastic scattering. This physical picture is also responsible for many other characteristic strong-field processes such as high-order harmonic generation [16] and high-order above-threshold ionization [17].

According to the recollision picture, NSDI probability will be largely suppressed under specific laser conditions, i.e., when using a circularly polarized light or increasing the laser wavelength. For circular polarization, the first tunneled electron tends to be spiraled away from the parent core by the additional transverse electric field component of the laser light, prohibiting the chance of recollision and thus NSDI yield. This has been verified by earlier measurements on rare-gas atoms using circularly polarized laser pulses [18,19]. However, later experiments on NO, O_2 molecules [20], and Mg atoms [21] discovered unexpected enhanced double ionization for circular polarization. These surprising experimental observations have stimulated a number of classical or semiclassical simulations that all incorporate recollision mechanics [22–28]. In these theoretical descriptions, a set of special electron trajectories turns out to drive the recollision process even for circular polarization and the occurrence of these trajectories critically depends on the atomic or molecular species [23,24].

Another important influence on NSDI involves the laser wavelength. This is due to the fact that the propagation time of the electron related to the spreading of the electron wave packet is proportional to the driving wavelength. Therefore, the electron recollision probability significantly decreases when increasing the wavelength. Additionally, upon

*H.Kang@gsi.de

recollision, the returning electron possibly induces an impact direct ionization, i.e., $(e, 2e)$ process or an excitation with subsequent ionization (ESI) [29–32]. The cross section of impact ionization or excitation sensitively depends on the electron impact energy, which has a maximum value of $3.17U_p$. Here U_p is the ponderomotive energy $U_p \propto \lambda^2 I$, where λ is the laser wavelength and I is the laser intensity. Experimentally, the wavelength (up to 2300 nm) dependence of Xe double ionization has been investigated in Ref. [33]. The authors showed that the ionic state excited by an electron impact process significantly contributes to the NSDI process. Another publication reported the intensity dependent nonsequential multiple ionization of Xe (up to Xe^{6+}) for even longer wavelengths at 3200 and 3600 nm [34]. It was revealed here that the electron impact direct ionization mainly contributes to the nonsequential multiple ionization of Xe. Similar studies have also been performed on Kr and Ne for ultraviolet wavelength [35]. Very recently, simulations accounting for both electron impact ionization and excitation cross sections were found to be able to quantitatively reproduce the experimental ratio of Ne^{2+}/Ne^{+} as function of intensity [36,37].

So far most previous atomic NSDI investigations concentrated on rare gases. Strong-field double ionization of alkaline-earth metal atoms offers an interesting alternative to those studies. They can be regarded as nearly ideal two-electron systems and contain a manifold of doubly excited states exhibiting a high degree of electron correlation. Among them, Mg has continued to attract significant attention in experiment [21,38–40] and theory [22–25,41–44], partially due to the interesting feature of NSDI with circular polarization. However, these studies were performed mainly for 800 nm or shorter wavelengths with the commonly used Ti:sapphire laser. The wavelength-dependent NSDI of Mg is less studied (see a theoretical publication [25] for an exception). Although the simulations based on recollision model reproduce the experimental results for 800 nm quantitatively or qualitatively [22–25], the influence of detailed electronic states on NSDI is generally ignored. To which extent the recollision scenario can be applied to NSDI of Mg is still far from understood. Considering the fact that Mg^{+} has a pretty rich electric structure, a central question is whether and how the ionic excited states are involved in NSDI of Mg.

Very recently, a joint experimental and theoretical investigation of the wavelength-dependent NSDI of Xe has been reported [45]. It was demonstrated that the wavelength scaling ratio of Xe^{2+}/Xe^{+} at fixed U_p can be explained by the interplay of wave-packet diffusion, Coulomb focusing, and a closely related Coulomb defocusing effect. In the current paper, we present a systematic investigation of wavelength scaling strong-field double ionization of Mg by linearly polarized light. We find a decrease of double ionization yield with increasing wavelength from 800–2000 nm, which is similar to Xe. Our data is well reproduced by a three-dimensional (3D) Monte Carlo simulation including recollision excitation cross section. The current work clearly identifies that the NSDI of Mg mainly occurs via the first ionic excited state $Mg^{+*}(3p^2P_{3/2,1/2})$ pumped by returning electron impact excitation process. While the direct ionization pathway plays a minor role here. Our work extends the strong-field double ionization experiments on Mg to the long wavelength limit and is beneficial for interpreting NSDI dynamics of alkaline-earth metal atoms.

This paper is organized as follows. In Sec. II we introduce the experimental apparatus. The theoretical model is described briefly in Sec. III. In Sec. IV we present and discuss the results, and the conclusions are drawn in Sec. V.

II. EXPERIMENTAL SETUP

In our experiments, the wavelength tunable midinfrared femtosecond laser pulses are generated by an optical parametric amplifier (OPA, TOPAS-C, Light Conversion, Inc.). The OPA is pumped by a commercial Ti:sapphire laser system (2.5 mJ, 40 fs, Legend, Coherent, Inc.) operated at 1 kHz [46]. The pulse durations are ~35 fs for 1250 ~ 1500 nm and ~45 fs for 1600 ~ 2200 nm. Before focused into the vacuum chamber, the pulse energy is variable by means of an achromatic half-wave plate followed by a polarizer. A homemade time-of-flight (TOF) mass spectrometer is used for measuring the ion signals. The details about the apparatus are described elsewhere [47,48]. By means of a turbomolecular pump and a cryopump, the base pressure achieved in the spectrometer is below 10^{-8} mbar. A collimated Mg atomic beam is produced by an electrically heated stainless atomic oven. The atomic density in ionization volume maintains stable during the measurements by continuously monitoring the temperature of the oven. Ions created in the ionization volume are detected by a microchannel plate located at the end of the spectrometer. The ion signal is then amplified, discriminated, and finally recorded by a multihit time digitizer to generate TOF mass spectra. The integrations of the counts detected for Mg^{+} and Mg^{2+} have been normalized to per laser shot and the ratio of Mg^{2+}/Mg^{+} is then determined. For high statistical accuracy, up to 10^6 laser shots are taken for lower intensities. The laser peak intensities for each wavelength are determined by comparing the measured saturation intensity of Xe^{+} yield with the Ammosov-Delone-Krainov (ADK) calculation [49]. The uncertainty of the intensity is estimated to be about 10%.

III. THEORETICAL MODEL

As mentioned above, the returning electron can induce an impact $(e, 2e)$ ionization or an ESI. Due to the diffusion of the electron wave packet, the recolliding wave packet can be very broad, especially for the long wavelengths used in the present work. The recollision-induced excitation or ionization probability thus depends on the impact parameter b. As proposed and experimentally verified in Ref. [34], the NSDI ratio is proportional to an effective, energy-averaged cross section and can be described by

$$R = \frac{\int dE\sigma(E)W_{\mathrm{ret}}(E)\frac{e^{-b^2/a_0^2}}{\pi a_0^2}}{\int dE W_{\mathrm{ret}}(E)}, \tag{1}$$

where $\sigma(E)$ is the field-free impact excitation or ionization cross section, which can be found from previous measurements on Mg with electron guns [50,51], $W_{\mathrm{ret}}(E)$ is the return energy distribution, and $a_0 = \sqrt{2/\triangle E}$, where $\triangle E$ is the excitation or ionization energy [31,32].

To calculate $W_{\rm ret}(E)$, we have performed a 3D Monte Carlo simulation. For each wavelength, an ensemble of 10^6 trajectories is randomly distributed in the time interval $-\pi/2 \leqslant \omega t_0 \leqslant \pi/2$ for a Mg atom, $I_p = 0.2811$ a.u. (7.646 eV). The electron trajectories at each time step during the laser pulse are calculated by solving $\frac{d^2\mathbf{r_i}}{dt^2} = -\mathbf{F}(t)$, where $\mathbf{F}(t) = \mathbf{F_0} f(t)\cos\omega t$ (ω is the laser frequency) is the laser field and the pulse envelope function $f(t)$ is a constant equal to 1 for the first ten cycles and reduced to 0 with three-cycle ramp in the form of $\cos^2$. We collect the trajectories return to the ionic core to obtain $W_{\rm ret}(E)$. To simulate the recollision impact excitation (ionization), the excitation (ionization) cross section, as a function of returning energy, for pumping ionic excited states (direct ionization) and the effective current density $\frac{e^{-b^2/a_0^2}}{\pi a_0^2}$ are taken into account [34]. For recollision-induced ESI, the excited states are assumed to be ionized subsequently with unity probability by the following laser fields [33,34]. The double ionization probability is thus related to the probability of the returning electron trajectories that induce efficient excitation or direct ionization. To this end, the impact parameter b and energy E for each returning trajectory is calculated and the weight of each trajectory is then multiplied by the corresponding excitation (ionization) cross section $\sigma(E)$ and effective current density $\frac{e^{-b^2/a_0^2}}{\pi a_0^2}$. A large number of these trajectories (about 5×10^5) are summed and thus the NSDI ratio can be calculated according to Eq. (1).

The initial conditions of the trajectories are defined according to tunneling ionization theory [52]. The tunneling exit point is determined by $z_0 = -I_p/F(t_0)$, where I_p is the first ionization potential of atoms and t_0 is the tunneling ionization instant of the electron. The electron is assumed to have zero initial longitudinal velocity and an initial transverse velocity v_{per} in the current studies. For each trajectory, the weight is evaluated by $w(t_0, v_{per}) = w(0)w(1)$ [53,54]:

$$w(0) = I_p C_{n^*l}^2 \left(\frac{2(2I_p)^{\frac{3}{2}}}{|F|}\right)^{2n^*-1} \exp[-2(2I_p)^{\frac{3}{2}}/3|F|] \qquad (2)$$

and

$$w(1) = \frac{(2I_p)^{\frac{1}{2}}}{|F|\pi} \exp\left[-v_{per}^2 (2I_p)^{\frac{1}{2}}/|F|\right], \qquad (3)$$

where $C_{n^*l} = (\frac{2e}{n^*})^{n^*} \frac{1}{\sqrt{2\pi n^*}}$ with the e constant and the effective principal quantum number $n^* = Z/\sqrt{2I_p}$, where Z is the nuclear charge.

IV. RESULTS AND DISCUSSION

Figures 1(a) and 1(b) display the measured yields of Mg^{2+} and Mg^+ as functions of intensity for 800 nm and 2000 nm, respectively. The intensity dependence of the results at 800 nm is in good agreement with previous experiments [21]. The Mg^{2+} yield increases continuously above $\sim 1.5 \times 10^{14}$ W/cm^2 due to the depletion of the Mg^+ for such high intensities, which is not seen for 2000 nm. This is probably because of the focal volume effect. In our experiments, the focus waist for 800 nm ($\sim$12.7 μm) is approximately equal to that for 2000 nm. Therefore, the focal volume is larger

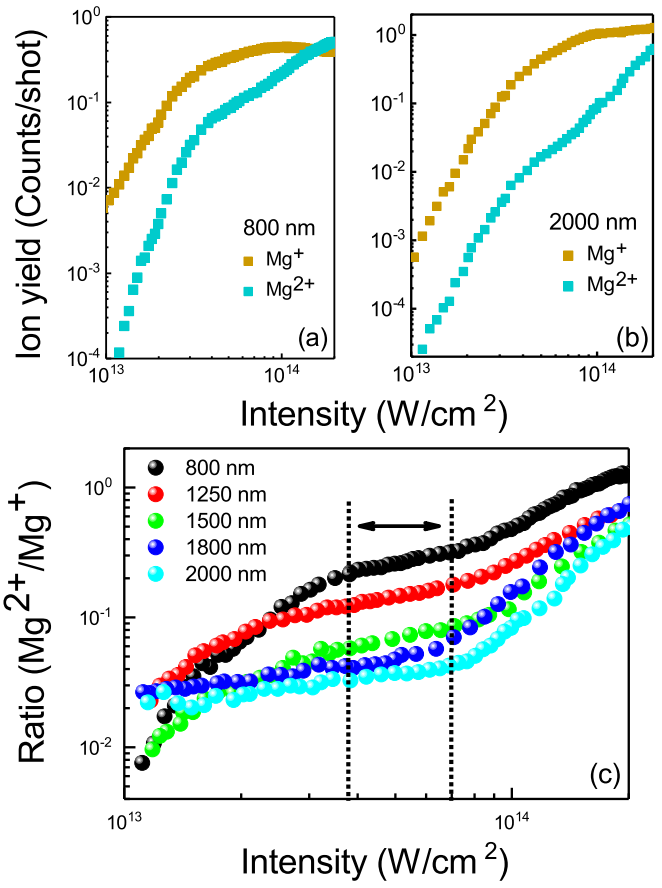

FIG. 1. (a) and (b) Measured Mg^{2+} and Mg^+ yields as functions of laser intensity for 800 nm and 2000 nm, respectively. (c) Experimental ratios of Mg^{2+}/Mg^+ as functions of laser intensity for various wavelengths. The dotted vertical lines mark the flat regions of the well-known knee structures for different wavelengths, which are suitable for studying the wavelength scaling.

for 800 nm, which results in the depletion of Mg^+ around 1.5×10^{14} W/cm^2 for 800 nm but not yet for 2000 nm.

At 2000 nm, for the first time, we observe a less pronounced knee structure indicating of NSDI below $\sim 8 \times 10^{13}$ W/cm^2. It is well known that the intensity dependence of the ratio between doubly charged and singly charged ions offers a more convenient criterion for discriminating NSDI and sequential double ionization (SDI) channel. In Fig. 1(c) we show the measured ratios of Mg^{2+}/Mg^+ as functions of intensity for various wavelengths ranging from 800–2000 nm. For each wavelength, an obvious knee shape can be identified at intensities below $\sim 8 \times 10^{13}$ W/cm^2, indicating NSDI channel mainly contribute to the production of Mg^{2+}. In the high-intensity region above $\sim 8 \times 10^{13}$ W/cm^2, the ratio curve increases fast with increase of the intensity, which means SDI channel dominates in the yield of Mg^{2+}. Furthermore, the NSDI yield decreases with increasing wavelength, which is similar to rare-gas atoms [45]. This feature implies that our observation might also be understood in the context of the recollision picture widely applied for rare gases, where the diffusion of the returning electron wave packet becomes stronger for longer wavelengths and suppresses the NSDI yield. To explore the wavelength scaling, we choose fixed

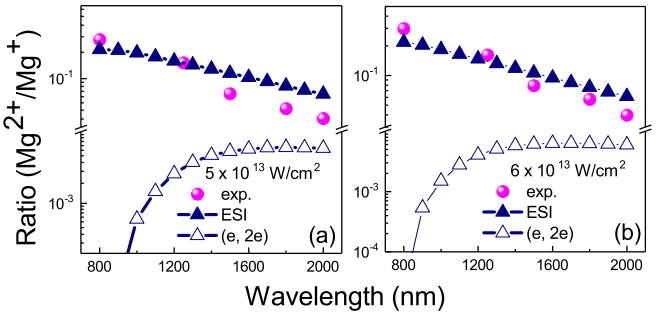

FIG. 2. (a) and (b) Experimental Mg^{2+}/Mg^{+} (the magenta dots) versus wavelength at fixed intensities of 5×10^{13} W/cm^2 and 6×10^{13} W/cm^2, respectively. The calculations considering recollision induced ESI (the solid triangles) and $(e, 2e)$ (the empty triangles) channels are shown separately for comparison. To compare with the data, the focal volume effect has been considered in the calculations. Note that a linear scale of the wavelength is employed.

intensities of 5 and 6×10^{13} W/cm^2, corresponding to the central part of the knee region, and plot the ratio of Mg^{2+}/Mg^{+} versus wavelength in Figs. 2(a) and 2(b), respectively. For other intensities located in the knee regime, we find similar dependence on the wavelength.

To simulate our data, we performed the model calculations as described in Sec. III. In our model, double ionization proceeds via either recollision impact $(e, 2e)$ ionization or ESI channel, as shown in Fig. 3. For the latter case, we only consider the lowest excited Mg^{+*} $3p$ states and they are assumed to subsequently ionize with unity probability during the following laser fields. For multicycle pulses as used in our experiments, the recollision-induced double ionization shows no obvious dependence on the pulse duration [30,55]. Although we did not experimentally test the dependence of Mg^{2+}/Mg^{+} on the pulse duration, one can expect no such dependence because NSDI of Mg in our present work can also be understood by the recollision picture.

The calculated results are shown in Figs. 2(a) and 2(b). One can find good agreement between the calculations considering recollision impact ESI channel and the experimental results for both intensities. The small discrepancies possibly arise from the errors caused by fitting the experimental excitation

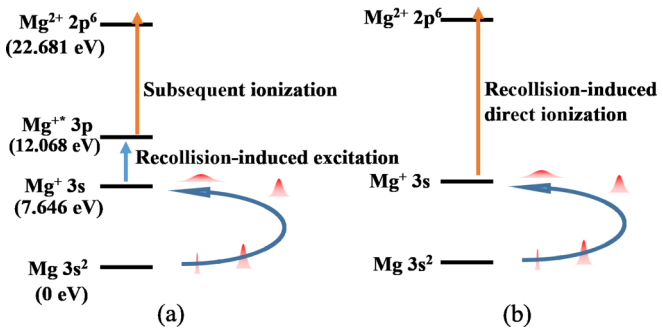

FIG. 3. Diagram of (a) recollision-induced ESI and (b) $(e, 2e)$ ionization channels leading to Mg^{2+}. For simplicity, only Mg^{+*} $3p$ state is considered in (a). The relevant energy levels are taken from NIST atomic database [56].

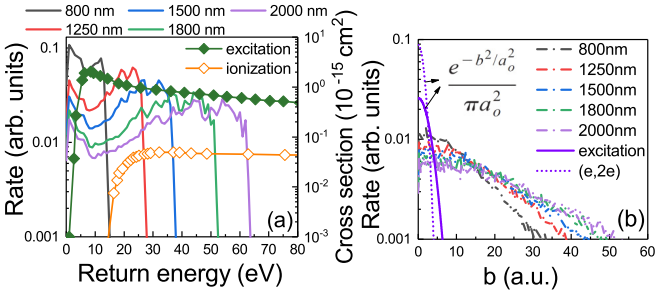

FIG. 4. (a) The returning energy distributions for various wavelengths at 5×10^{13} W/cm^2. The excitation (Mg^{+*} $3p$) and ionization cross sections used in our model simulations are shown for reference. The diamonds are the experimental measurements inferred from Refs. [50,51] while the lines are corresponding fittings. (b) The impact parameter distributions for various wavelengths at the same intensity as in (a). Each rate has been multiplied by a factor of 1.7×10^{-5} for comparison purposes. The focal volume effect has been considered in above calculations. Also shown is the effective current density of the returning electrons $\frac{e^{-b^2/a_0^2}}{\pi a_0^2}$ for excitation (the purple solid line) and $(e, 2e)$ process (the purple dotted line), respectively.

cross sections [Fig. 4(a)]. While the calculations considering $(e, 2e)$ process are much smaller than the experiments.

In Ref. [34], it was shown that the recollision impact direct ionization mainly contributes to the nonsequential multiple ionization of Xe leading to highly charged ions from Xe^{3+} to Xe^{6+} for two close wavelengths of 3200 nm and 3600 nm. For NSDI channel, it was found that the simulation for recollision impact ESI alone overestimates the experimental results. One possible reason is that the excitation cross section used in their calculation was scaled from the Lotz formula [57], which could introduce a minimum error of 25% [34]. In the current work we study the dependence of NSDI of Mg on the wavelength between 800 nm and 2000 nm. Following the simulation method in Ref. [34], the excitation and ionization cross sections used here are obtained from the experiments reported in Refs. [50,51]. Our simulation considering recollision impact ESI alone reproduces the observation well. We thus conclude that the observed NSDI of Mg is mainly due to the recollision impact excitation via the first excited states of Mg^{+}. This clearly justifies the key role of the ionic excited states during the double ionization of Mg.

Our observations are closely related to the returning energy distributions and the diffusion of the electron wave packet upon recollision, both depending on the wavelength sensitively. In Figs. 4(a) and 4(b) we present the calculated returning energy distributions and the impact parameter b distributions for various wavelengths at 5×10^{13} W/cm^2, respectively. The calculations for 6×10^{13} W/cm^2 show similar features. The used excitation and ionization cross sections taken from previous experiments [50,51] are also shown for comparison in Fig. 4(a). The excitation cross section is about one order of magnitude larger than the ionization cross section for energies above 25 eV. For lower energies, the ionization cross section becomes even smaller by several orders of magnitude. This is the reason why the calculation for $(e, 2e)$ process is much smaller than that for recollision-induced ESI. For every wavelength, the energy distribution in the

high-energy region arises continuously to a peak with a cutoff. Due to the existence of the tunneling exit, the cutoff position is slightly larger than $3.17U_p$. From Fig. 4(a), one can see that the excitation cross section continues to decrease for higher energies above 10 eV. The returning energy distributions get broader and peak at larger values well above 10 eV for longer wavelengths. This gives rise to the decrease of the recollision-induced ESI with increasing wavelengths.

Another key factor is the diffusion effect of the returning electron wave packet, which gets stronger when the wavelength is increased [Fig. 4(b)]. The recollision-induced excitation process depends on b^2 exponentially [Eq. (1)]. The term $\frac{e^{-b^2/a_0^2}}{\pi a_0^2}$ in Eq. (1) describes the effective current density of the returning electrons, which defines a window of b for efficient impact excitation or ionization, see Fig. 4(b). The density of the returning electrons within the excitation window decreases for longer wavelengths, indicating that the ESI ratio drops monotonically with increasing wavelength. This also holds true for $(e, 2e)$ process. However, the recollision-induced ionization cross section increases extremely fast when the wavelength is increased from 800–1250 nm, and becomes flat when the wavelength is further increased [Fig. 4(a)]. Consequently, the calculated Mg^{2+}/Mg^{+} for $(e, 2e)$ process first increases very rapidly until 1250 nm and then decreases slowly when the wavelength is further increased [Fig. 2(a)].

So far we have shown that NSDI of Mg mainly occurs via the recollision impact ESI channel. This mechanism is expected to be valid for other alkaline-earth metals due to their similar electronic structures. While a number of experiments on other alkaline-earth metals performed with visible ns or ps laser pulses has been reported [58–60], there is a lack of strong-field double ionization measurements with fs pulses. We hope that the current work will prompt further researches along this direction. In particular, the double ionization of Ca atoms by fs laser pulses was shown to be enhanced by a resonance control scheme via a transient excitation of doubly excited states [61,62]. In our current work, NSDI of Mg mainly occurs via the transient excitation to the intermediate excited states of Mg^{+}. Similarly, it is promising to control the Mg^{2+} production by adjusting the transient population of Mg^{+*}, which can be done by varying laser parameters.

Very recently, a laser-induced inelastic diffraction scheme based on the NSDI occurring through $(e, 2e)$ process has been proposed [63]. It was realized in the kinematically complete experiments on Xe and Ar. The doubly differential cross section can be reliably extracted from the two-dimensional photoelectron momentum distributions from the NSDI process. This scheme can also be applied to Mg. Here the information on the differential excitation cross section is possibly accessed by similar methods. Since the NSDI of Mg is relevant to the recollision ESI mechanism, the emission angle resolved electrons coincident with Mg^{2+} possibly encode dynamical information of the intermediate excited states involved. To this end, the differential measurements on double ionization of Mg are required. This holds a promise to resolve the ultrafast evolution of the ionic excited states during NSDI process of atomic or molecular targets with complex electronic structures.

V. CONCLUSION

In conclusion, we report a systematic investigation of wavelength scaling of strong-field double ionization of Mg by linearly polarized light. We find a decrease of double ionization yield with increasing wavelength ranging from 800–2000 nm, which is similar to rare-gas atoms. Our observation is satisfyingly reproduced by a 3D Monte Carlo simulation considering recollision excitation cross section. The current studies clearly identify that the NSDI of Mg mainly occurs via the ionic excited state $Mg^{+*}(3p^2P_{3/2,1/2})$ pumped by returning electron impact process, while the direct ionization pathway plays a minor role. The wavelength dependence of NSDI ratio is due to the recollision energy-dependent excitation cross section as well as the electron wave packet diffusion effects, both depending on the wavelength crucially. Our work represents a step towards strong-field double ionization experiments on alkaline-earth metal atoms in the long wavelength limit and sheds light on the underlying mechanism of NSDI for such atoms.

ACKNOWLEDGMENTS

We thank Philipp Wustelt and Gerhard G Paulus for valuable and stimulating discussions. The work is supported by the National Natural Science Foundation of China (No. 11425414, No. 11834015, No. 11847243, and No. 11804374) and National Key program for S&T Research and Development (No. 2016YFA0401100).

[1] R. Dörner, Th. Weber, M. Weckenbrock, A. Staudte, M. Hattass, H. Schmidt-Böcking, R. Moshammer, and J. Ullrich, Adv. At. Mol. Opt. Phys. **48**, 1 (2002).

[2] W. Becker, X. J. Liu, P. J. Ho, and J. H. Eberly, Rev. Mod. Phys. **84**, 1011 (2012).

[3] A. l'Huillier, L. A. Lompre, G. Mainfray, and C. Manus, Phys. Rev. A **27**, 2503 (1983).

[4] D. N. Fittinghoff, P. R. Bolton, B. Chang, and K. C. Kulander, Phys. Rev. Lett. **69**, 2642 (1992).

[5] B. Walker, B. Sheehy, L. F. DiMauro, P. Agostini, K. J. Schafer, and K. C. Kulander, Phys. Rev. Lett. **73**, 1227 (1994).

[6] S. Augst, A. Talebpour, S. L. Chin, Y. Beaudoin, and M. Chaker, Phys. Rev. A **52**, R917 (1995); A. Talebpour, C.-Y. Chien, Y. Liang, S. Larochelle, and S. L. Chin, J. Phys. B **30**, 1721 (1997).

[7] A. S. Alnaser, T. Osipov, E. P. Benis, A. Wech, B. Shan, C. L. Cocke, X. M. Tong, and C. D. Lin, Phys. Rev. Lett. **91**, 163002 (2003).

[8] C. Cornaggia and Ph. Hering, Phys. Rev. A **62**, 023403 (2000).

[9] D. Zeidler, A. Staudte, A. B. Bardon, D. M. Villeneuve, R. Dörner, and P. B. Corkum, Phys. Rev. Lett. **95**, 203003 (2005).

[10] E. Eremina, X. Liu, H. Rottke, W. Sandner, M. G. Schätzel, A. Dreischuh, G. G. Paulus, H. Walther, R. Moshammer, and J. Ullrich, Phys. Rev. Lett. **92**, 173001 (2004).

[11] Th. Weber, H. Giessen, M. Weckenbrock, G. Urbasch, A. Staudte, L. Spielberger, O. Jagutzki, V. Mergel, M. Vollmer, and R. Dörner, Nature (London) **405**, 658 (2000).

[12] Th. Weber, M. Weckenbrock, A. Staudte, L. Spielberger, O. Jagutzki, V. Mergel, F. Afaneh, G. Urbasch, M. Vollmer, H. Giessen, and R. Dörner, Phys. Rev. Lett. **84**, 443 (2000).

[13] R. Moshammer, B. Feuerstein, W. Schmitt, A. Dorn, C. D. Schröter, J. Ullrich, H. Rottke, C. Trump, M. Wittmann, G. Korn, K. Hoffmann, and W. Sandner, Phys. Rev. Lett. **84**, 447 (2000).

[14] A. Rudenko, K. Zrost, B. Feuerstein, V. L. B. de Jesus, C. D. Schröter, R. Moshammer, and J. Ullrich, Phys. Rev. Lett. **93**, 253001 (2004).

[15] P. B. Corkum, Phys. Rev. Lett. **71**, 1994 (1993).

[16] A. D. Shiner, B. E. Schmidt, C. Trallero-Herrero, H. J. Wörner, S. Patchkovskii, P. B. Corkum, J. C. Kieffer, F. Légaré, and D. M. Villeneuve, Nature Phys. **7**, 464 (2011).

[17] G. G. Paulus, W. Nicklich, H. Xu, P. Lambropoulos, and H. Walther, Phys. Rev. Lett. **72**, 2851 (1994).

[18] B. Walker, E. Mevel, Baorui Yang, P. Breger, J. P. Chambaret, A. Antonetti, L. F. DiMauro, and P. Agostini, Phys. Rev. A **48**, R894 (1993).

[19] P. Dietrich, N. H. Burnett, M. Ivanov, and P. B. Corkum, Phys. Rev. A **50**, R3585 (1994).

[20] C. Guo, M. Li, J. P. Nibarger, and G. N. Gibson, Phys. Rev. A **58**, R4271 (1998); C. Guo and G. N. Gibson, *ibid.* **63**, 040701 (2001).

[21] G. D. Gillen, M. A. Walker, and L. D. Van Woerkom, Phys. Rev. A **64**, 043413 (2001).

[22] F. Mauger, C. Chandre, and T. Uzer, Phys. Rev. Lett. **105**, 083002 (2010).

[23] L. B. Fu, G. G. Xin, D. F. Ye, and J. Liu, Phys. Rev. Lett. **108**, 103601 (2012).

[24] A. Kamor, F. Mauger, C. Chandre, and T. Uzer, Phys. Rev. Lett. **110**, 253002 (2013).

[25] N. Li, Y. Zhou, X. Ma, M. Li, C. Huang, and P. Lu, J. Chem. Phys. **147**, 174302 (2017).

[26] X. Wang and J. H. Eberly, New J. Phys. **12**, 093047 (2010).

[27] X. Wang and J. H. Eberly, Phys. Rev. Lett. **105**, 083001 (2010).

[28] S. Ben, P. Y. Guo, K. L. Song, T. T. Xu, We. W. Yu, and X. S. Liu, Opt. Express **25**, 1288 (2017).

[29] X. L. Hao, J. Chen, W. D. Li, B. Wang, X. Wang, and W. Becker, Phys. Rev. Lett. **112**, 073002 (2014).

[30] V. R. Bhardwaj, S. A. Aseyev, M. Mehendale, G. L. Yudin, D. M. Villeneuve, D. M. Rayner, M. Yu. Ivanov, and P. B. Corkum, Phys. Rev. Lett. **86**, 3522 (2001).

[31] G. L. Yudin and M. Y. Ivanov, Phys. Rev. A **63**, 033404 (2001).

[32] X. M. Tong, Z. X. Zhao, and C. D. Lin, Phys. Rev. A **68**, 043412 (2003).

[33] G. Gingras, A. Tripathi, and B. Witzel, Phys. Rev. Lett. **103**, 173001 (2009).

[34] A. D. DiChiara, E. Sistrunk, C. I. Blaga, U. B. Szafruga, P. Agostini, and L. F. DiMauro, Phys. Rev. Lett. **108**, 033002 (2012).

[35] N. Ekanayake, Sui Luo, B. L. Wen, L. E. Howard, S. J. Wells, M. Videtto, C. Mancuso, T. Stanev, Z. Condon, S. LeMar, A. D. Camilo, R. Toth, W. B. Crosby, P. D. Grugan, M. F. Decamp, and B. C. Walker, Phys. Rev. A **86**, 043402 (2012).

[36] Z. Chen, X. Li, O. Zatsarinny, K. Bartschat, and C. D. Lin, Phys. Rev. A **97**, 013425 (2018).

[37] Z. Chen, L. Zhang, Y. Wang, O. Zatsarinny, K. Bartschat, T. Morishita, and C. D. Lin, Phys. Rev. A **99**, 043408 (2019).

[38] D. Kim, S. Fournier, M. Saeed, and L. F. DiMauro, Phys. Rev. A **41**, 4966 (1990).

[39] D. Xenakis, N. E. Karapanagioti, D. Charalambidis, H. Bachau, and E. Cormier, Phys. Rev. A **60**, 3916 (1999).

[40] I. Liontos, A. Bolovinos, S. Cohen, and A. Lyras, Phys. Rev. A **70**, 033403 (2004).

[41] T. Nakajima and G. Buica, Phys. Rev. A **74**, 023411 (2006).

[42] N. I. Shvetsov-Shilovski, D. Dimitrovski, and L. B. Madsen, Phys. Rev. A **85**, 023428 (2012).

[43] H.-P. Kang, S.-P. Xu, Y.-L. Wang, S.-G. Yu, X.-Y. Zhao, X.-L. Hao, X.-Y. Lai, T. Pfeifer, X.-J. Liu, J. Chen, Y. Cheng, and Z.-Z. Xu, J. Phys. B **51**, 105601 (2018).

[44] N. I. Shvetsov-Shilovski, M. Lein, and L. B. Madsen, Phys. Rev. A **98**, 023406 (2018).

[45] Y. L. Wang, S. P. Xu, Y. J. Chen, H. P. Kang, X. Y. Lai, W. Quan, X. J. Liu, X. L. Hao, W. D. Li, S. L. Hu, J. Chen, W. Becker, W. Chu, J. P. Yao, B. Zeng, Y. Cheng, and Z. Z. Xu, Phys. Rev. A **95**, 063415 (2017).

[46] Y. Fu, H. Xiong, H. Xu, J. Yao, Y. Yu, B. Zeng, W. Chu, X. Liu, J. Chen, Y. Cheng, and Z. Xu, Phys. Rev. A **79**, 013802 (2009).

[47] Z. Y. Lin, X. Y. Jia, C. L. Wang, Z. L. Hu, H. P. Kang, W. Quan, X. Y. Lai, X. J. Liu, J. Chen, B. Zeng, W. Chu, J. P. Yao, Y. Cheng, and Z. Z. Xu, Phys. Rev. Lett. **108**, 223001 (2012).

[48] H. P. Kang, Z. Y. Lin, S. P. Xu, C. L. Wang, W. Quan, X. Y. Lai, X. J. Liu, X. Y. Jia, X. L. Hao, J. Chen, W. Chu, J. P. Yao, B. Zeng, Y. Cheng, and Z. Z. Xu, Phys. Rev. A **90**, 063426 (2014).

[49] S. Larochelle, A. Talebpoury, and S. L. Chin, J. Phys. B **31**, 1201 (1998).

[50] I. P. Zapesochnyi, V. A. Kel'man, A. I. Imre, A. I. Dashchenko, and F. F. Danch, Zh. Eksp. Teor. Fiz. **69**, 1948 (1975) [Sov. Phys. JETP **42**, 989 (1975)].

[51] C. Becker, H. Knopp, J. Jacobi, H. Teng, S. Schippers, and A. Muller, J. Phys. B **37**, 1503 (2004).

[52] N. B. Delone and V. P. Krainov, J. Opt. Soc. Am. B. **8**, 1207 (1991).

[53] A. M. Perelomov, V. S. Popov, and M. V. Terentev, J. Exptl. Theoret. Phys. (U.S.S.R.) **50**, 1393 (1966) [Sov. Phys. JETP **23**, 924 (1966)].

[54] M. V. Ammosov, N. B. Delone, and V. P. Krainov, Zh. Eksp. Teor. Fiz. **91**, 2008 (1986) [Sov. Phys. JETP **64**, 1191 (1986)].

[55] P. J. Ho and J. H. Eberly, Phys. Rev. Lett. **95**, 193002 (2005).

[56] https://physics.nist.gov/PhysRefData/ASD/levels_form.html

[57] W. Lotz, Z. Phys. **206**, 205 (1967).

[58] I. I. Bondar and V. V. Suran, Pis'ma Zh. Eksp. Teor. Fiz. **56**, 78 (1992) [JETP Lett. **56**, 78 (1992)]; Zh. Eksp. Teor. Fiz. **103**, 774 (1993) [JETP **76**, 381 (1993)].

[59] I. I. Bondar, V. V. Suran, and M. I. Dudich, J. Phys. B **33**, 4243 (2000).

[60] I. I. Bondar, V. V. Suran, and D. I. Bondar, Phys. Rev. A **88**, 023407 (2013).

[61] E. Papastathopoulos, M. Strehle, and G. Gerber, Chem. Phys. Lett. **408**, 65 (2005).

[62] M. Sukharev, E. Charron, and A. Suzor-Weiner, Phys. Rev. A **66**, 053407 (2002).

[63] W. Quan, X. L. Hao, X. Q. Hu, R. P. Sun, Y. L. Wang, Y. J. Chen, S. G. Yu, S. P. Xu, Z. L. Xiao, X. Y. Lai, X. Y. Li, W. Becker, Y. Wu, J. G. Wang, X. J. Liu, and J. Chen, Phys. Rev. Lett. **119**, 243203 (2017).